International Conference on Space Optics—ICSO 2022

Dubrovnik, Croatia

3–7 October 2022

Edited by Kyriaki Minoglou, Nikos Karafolas, and Bruno Cugny,

ICSO 2022
International Conference on Space Optics
3 – 7 October 2022 | Dubrovnik | Croatia

Development of a compact and agile 400 mJ, 100 Hz amplifier for spaceborne applications

esa icso proceedings cnes

International Conference on Space Optics — ICSO 2022, edited by Kyriaki Minoglou, Nikos Karafolas,
Bruno Cugny, Proc. of SPIE Vol. 12777, 127770P · © 2023 ESA and CNES · 0277-786X · doi: 10.1117/12.2688838

Development of a compact and agile 400 mJ, 100 Hz amplifier for spaceborne applications

Rapaport Alexandra[*a], Fretel Emmanuel[a], Philippe Becerril[a], Aubry Chloé[a], Meyer Virgile[a], Montagne Jean-Eucher[a], Speiser Jochen[b], Papayannis Alex[c], Ribes Pol[d], Tzeremes Georgios[d]
[a]CILAS ArianeGroup, 8 avenue Buffon, 45000 Orléans, France; [b]Institute of Technical Physics – DLR, Pfaffenwaldring 38-40, 70569 Stuttgart, Germany; [c]National Technical University of Athens, Zografou Campus, 9, Iroon Polytechniou str, 15780 Zografou, Greece; [d]European Space Agency, Keplerlaan 1, 2201 AZ Noordwijk, The Netherlands

ABSTRACT

We have improved on the characteristics of a diode-pumped, 1064-nm amplifier. The system can deliver 400 mJ @ 100 Hz with very limited wavefront distortion due to thermal effects. It follows that the amplifier can be powered on and reach full energy in a few seconds.

The amplifier stable long thermal lens ensures that optical elements used downpath (potentially non-linear crystals for frequency conversion, or a telescope) are at no risk of laser damage, even during the short warm-up time. Additionally, the amplifying system can be operated at any repetition rate up to 100 Hz, and at any energy level, without having to adjust the hardware. The ease of operation, and number of shots saved on the diode lifetime can be a critical advantage in space.

The amplifier pumping design enables duplication of the pump source with only 3% increase of the system mass: the doubling of the stacks does not require any additional optical component, nor any moving part. With solar radiation, the diode stacks are among the weakest link of the system, so this unique property is valuable for space applications.

The laser amplifier was set-up and characterized as a laboratory breadboard, and a CAD version of a robust system was drawn and analyzed. We will review the properties of this compact amplifying system. Due to its uniform output beam distribution, it is very well suited for non-linear frequency conversion, and for long-range space applications.

Keywords: optical amplifier, thermal lensing, pump source redundancy

1. INTRODUCTION

In order to accrue its current knowledge and understanding of the Earth system and its processes, the European Space Agency (ESA) has started the Living Planet Program (LPP). This program regroups the launch of several satellites, each one being dedicated to a specific area of measurements. Magnetic field, ice cover, soil moisture, carbon stored in land forests, gravity field, …: the breakthrough techniques dedicated to these subjects identified as key by the scientific community will enable the acquisition of the exact data required by the user, and lead to a better prediction of the effects a changing climate may bring. In that scope, the Earth Explorer Atmospheric Dynamics Mission Aeolus mission was selected to provide global observations of wind profiles from space to improve the quality of weather forecasts, and to advance the understanding of atmospheric dynamics and climate processes. It relies on a single active Doppler Wind Lidar (DWL) instrument (ALADIN) in order to measure both Rayleigh scattering from atmospheric molecules, and Mie scattering from aerosols and cloud particles. ALADIN is one of the most sophisticated instruments ever to be put into orbit, and DWL is the only method that has the potential to provide the required data globally, from direct wind observations. Obtaining the wind velocity information from tropical regions is critical for improving weather forecasting, and for getting accurate meteorological models. The improved numerical predictions will enable a better understanding of atmospheric dynamics, and enrich climate research.

[*] rapaport@cilas.com; https://cilas.ariane.group/en/

ALADIN consists of a laser source, a 1.5m-telescope, and a combined receiver assembly for Mie (Fizeau interferometer), and for Rayleigh (Fabry-Perot interferometer) scattering. The spacecraft used is a new design, but the platform is based on a heritage from other ESA missions developed by Airbus DS (CryoSat, Rosetta).

The ADM-Aeolus mission, which was launched in August 2018, has suffered several delays caused by the difficulties encountered during the development of the laser source. The main issues that had to be resolved before sending ALADIN to space were the mechanical stability of the system, and the lifetime of the optical elements integrated in the laser source. Indeed, the choice of Ultra-Violet (UV) radiation for the useful beam in order to improve on the amount of back-scattering, combined with a system pumped down to vacuum pressure, caused recurring Laser Induced Contamination (LIC) problems. Additionally, the fluence reached along the beam path comes close to the limits that state-of-the-art surface treatments can withstand. Improving coating techniques to increase Laser Induced Damage Threshold (LIDT), and controlling the laser thermal lensing to prevent changes in the beam distribution, were critical for the validation of the mission launch. The resolution of these technical issues generated breakthrough knowledge about the causes of surface optical damages. Still, controlling the thermal lensing of the laser in order to preserve safe operation of the system from cold-start to continuous operation, reveals challenging with the laser design chosen.

This problematic has led ESA to start new programmes to mitigate thermal lensing in the laser system. A General Support Technology Programme (GSTP) was selected to develop an elegant compact breadboard of a 10-mJ, 100-Hz oscillator showing low thermal lensing and low heat generation inside the active material. This program called Q-switched Optical Master Oscillator II (QOMA II) relies on long wavelength pumping of a multi-segmented Nd:YAG crystal to decrease thermal load. A Technology Research Programme (TRP) was selected to investigate an innovative architecture for the 400-mJ, 100-Hz, 1064-nm amplifier, based on thick disks and having very weak thermal distortions.

Very promising results at 50 Hz were obtained by the end of this program in 2018, so follow-up programmes were launched in order to improve on the amplifier building blocks. We report here on the latest results achieved in the development of this thick disks amplifier.

2. AMPLIFIER ARCHITECTURE

In the ALADIN instrument, the amplifier output radiation goes through frequency conversion crystals that generate a 355-nm beam, which is then directed towards Earth through the large telescope. The quantity that is measured by the instrument is the frequency shift of the backscattered UV light as a function of time (i.e. altitude of the backscatterer). The shift is directly linked to the velocity of the back-scatterer through the Doppler effect, so wind distribution and particles displacement can be characterized from space. For typical atmospheric data, Doppler frequency shifts to be detected are on the order of 10^8 smaller than the frequency of the emitted UV light. This implies a very narrow and stable spectral line, so requirements are for a linewidth less than 50 MHz. and frequency jitter pulse to pulse better than 10 MHz rms.

To achieve the spectral characteristics required for ALADIN, a frequency-stabilized, single longitudinal mode, low-power, cw Neodymium doped Yttrium Aluminum Garnet (Nd:YAG) laser is used to seed a 5-mJ, 50-Hz, Q-switched master oscillator. This seed laser is not available to us at this time, so an in-house Q-switched, 20-ns pulse duration, Nd:YAG laser operating at 100 Hz was used to inject the amplifier.

The amplifier is based on active mirror technology, where pumped Nd:YAG disks are set-up to reflect the injection beam so that it is amplified from one disk to the next, as illustrated in Figure 1[]. A High-Reflectivity (HR) mirror enables double pass through the disks, which increases the system efficiency. Pump radiation is injected through the dichroic mirror and enters the disks through their front face.

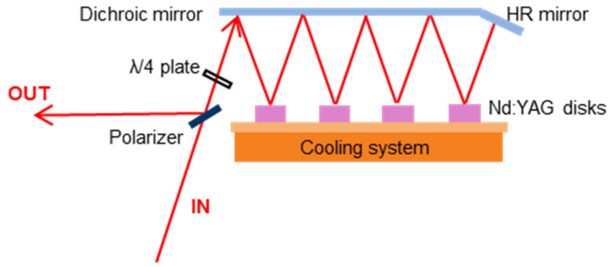

Figure 1: Amplification module based on active mirror technology.

Most active mirror lasers are made of thin-disks that take advantage of the reduced thermal resistance of the short path between the front and back face of the disk (usually a few hundred microns). Because the disks are so thin, absorption of the pump radiation is not very efficient, so large dopant concentrations are necessary, as well as a regenerative pump design. Large dopant concentrations are achievable with Ytterbium (Yb^{3+}) dopants, so most disk lasers are Yb lasers, which are very sensitive to temperature. Indeed, Yb^{3+} lasers are 3-level lasers, and the laser transition terminates in the ground state manifold. Thermal population of the laser final energy level is detrimental, so those lasers require low temperature cooling to operate efficiently.

The amplifier in our case is based on Nd^{3+}. The highest Nd^{3+} concentration that does not result in degraded optical properties in YAG is 1.2% Nd^{3+}. To achieve good 808-nm pump absorption through the disks (>95%) at this concentration, they must be at least 3.4 mm-thick. YAG is one of the better crystals for thermal conductivity as far as laser materials go. Still, when operating at 100 Hz with 3.4 mm thick disks, the temperature elevation of the uncooled, front face of the disk can be detrimental to the laser performance (spectral shift of the emission line through the disk, decrease of the Nd^{3+} emission cross-section, stress induced birefringence, all lead to efficiency loss). We therefore designed the amplifier with 3.4-mm thick disks and dimensioned the pump module and optical elements to achieve 400-mJ while limiting the front-face temperature elevation.

The 400-mJ amplifier consists of 2 amplification stages with similar architecture. The pump modules rely on microlens arrays so the diode stacks used have to be Fast Axis Collimated (FAC). The principle of flat top illumination using 2 microlens arrays is shown Figure 2.

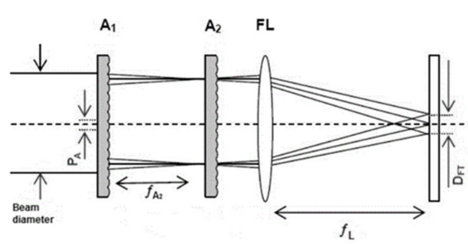

Figure 2: Flat-top illumination using microlens arrays.

In order to achieve compactness of the micro-optics arrays (hence good pump coupling efficiency), hexagonal shaped lenses are chosen, which leads to a hexagonal shaped, uniform illumination of the disks. A typical pump distribution at the disks is simulated and measured as shown in Figure 3.

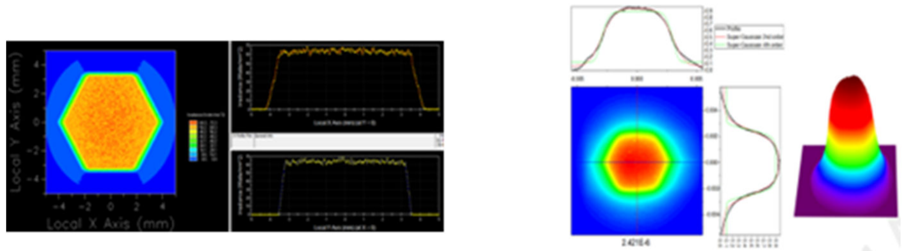

Figure 3: Pump distribution at the disk. Left: simulated in FRED® software. Right: Measured with Ophir-Spiricon beam profiler.

The laser beam is injected in the 2 amplification stages through a Thin Film Polarizer (TFP), and a QuarterWave Plate (QWP) placed before the HR back mirror makes it possible to out-couple the amplified beam through polarization. A 3D lay-out of the complete amplification system is shown Figure 4, along with a picture of the laboratory set-up.

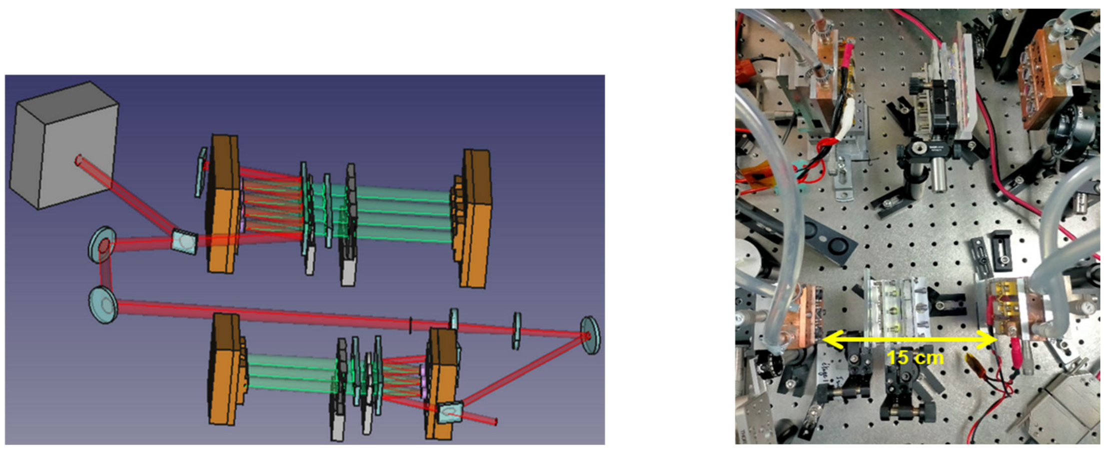

Figure 4: 3D layout and laboratory set-up picture of the 400-mJ amplifier.

The pump emission irradiates the disks after going through a rectangular-shape, dichroic mirror that is ~25 mm high, and can be about 90 mm long for the amplifier second stage. This mirror reflects the amplified beam from disk to disk in a zigzag fashion. In order to avoid Parasitic Lasing (PL), the mirror cannot reflect 1064 nm radiation in the zones directly located in front of the pump disks. Therefore, it consists of several zones, alternating HR and Anti-Reflection (AR) coated sections. This multizone mirror is produced by a process of photolithography, where a photoresin is deposited to mask half the zones during a first coating run, then removed, before the second coating run is done.

3. RECENT DEVELOPMENTS

The 400-mJ amplifier was characterized in 2018 at 50 Hz, and showed singular properties that warranted further development [2]. In particular, we demonstrated good efficiency (22.7% Optical-to-Optical (O2O) efficiency), and very low thermal lensing effect (about 0.01 diopter) when operating at 400 mJ, 50 Hz. This minute thermal lensing enables a warm-up time of less than 5 seconds to reach 99% full energy.

Thermal lensing puts the optical elements in the laser path at risk of optical damage if it varies during operation. A change in repetition rate or pump energy, and the waist of the amplified beam could be located on an optical surface and cause laser damage. CILAS amplifier exhibits almost no thermal lensing for any pumping condition, with no active element, so it is simple and safe to operate.

Control of thermal lensing is obtained by functionalizing the disks so that wavefront distortions due to pump absorption are compensated over the amplified beam area. In the latest work, we have demonstrated improved control of the distortions using a space compatible polyurethane coating qualified by the Centre National d'Etudes Spatiales.(CNES). We also upgraded the adhesive used to assemble the Nd:YAG disks to their cooling interface with a NASA qualified epoxy. With only low outgassing materials now used in the amplifier, we have refined our functionalization process. We now consistently obtain wavefront distortions caused by pumping functionalized single elements, that are less than 0.02λ rms over the beam area, and that are independent of the average pump power absorbed. The flatness of the reflected wavefront is illustrated Figure 5 for disks of both stages.

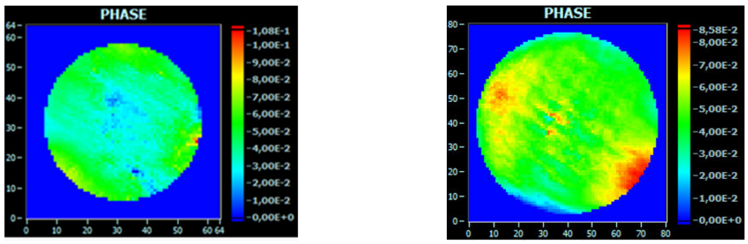

Figure 5: Wavefront measurement (with Phasics SID4 sensor and software) of a plane wave after reflection through a pumped functionalized Nd:YAG disk. Left: stage 1 disk. Right: Stage 2 disk.

This in an improvement over the original breadboard. In the first set-up, stage 2 disks caused some astigmatism of the reflected wavefront, which presented a Peak-to-Valley (P2V) larger than 0.1λ. This explained the difference in the beam M² value measured over the X ($M^2_x = 3.3$) and Y ($M^2_y = 2.7$) directions. The beam obtained at 50 Hz is shown in Figure 6. We expect an improved beam quality with this second generation breadboard.

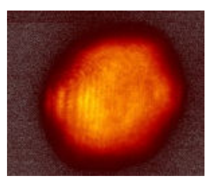

Figure 6: Output beam distribution at 400 mJ, 50 Hz.

A CAD drawing of an elegant breaboard was realized and analyzed for resistance to shocks and vibrations. Compact and robust optomechanical mounts were created that are designed to enable fine tuning of the optics, followed by a definite positioning using mechanical parts to avoid possible displacements after the optics are set. A view of the first amplifier stage is given Figure 7.

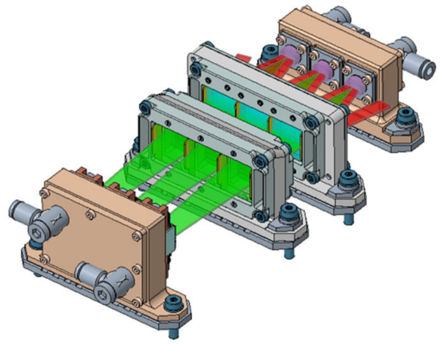

Figure 7: Optomechanical design of amplifier stage 1

A choice was made to place the 2 amplification stages on either side of a central vertical plate. This facilitates access to the optics in both stages while minimizing the amplifier footprint. A mechanical analysis was realized on this elegant breadboard with the assumption that the material used for the mechanical parts is 6061 T6 aluminum.

The modal analysis, done with NX software, showed that for stage 1 optical mounts, all eigenmodes have eigenfrequency above the highest frequency found in typical launch profiles spectrum (2000 Hz, value provided by ESA). Stage 2 optical mounts are larger, and the calculated eigenfrequencies are smaller. Some optimization is still necessary for some of the mounts to satisfy ESA requirements entirely.

The modal analysis for the complete system showed low frequency modes that were eliminated by adding some stiffeners, ribs, and columns to attach the casing. Temperature sensors were also placed in the CAD drawing. The resulting elegant breadboard is shown Figure 8, along with the main dimensions. A footprint of 289 mm x 131 mm is obtained for the amplifier, with a height of 235 mm. Total mass including a commercial optical isolator inserted between the 2 stages is 4.8 kg.

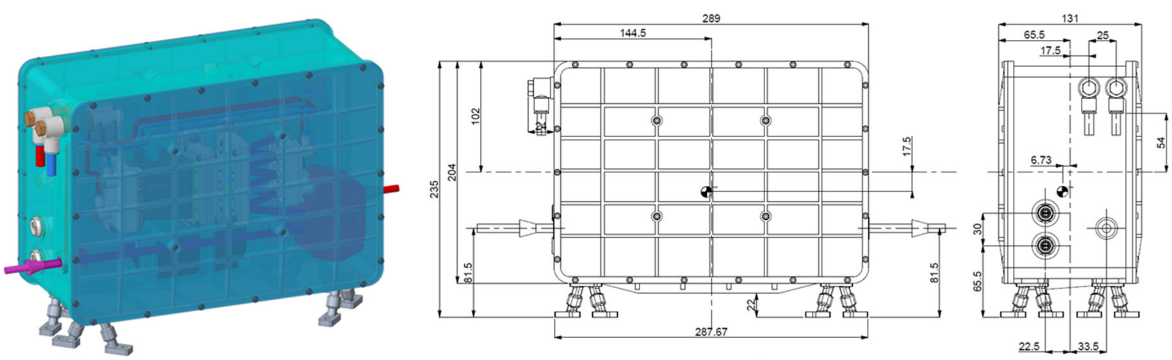

Figure 8: CAD drawing of the elegant breadboard, with main dimensions

Some hypotheses that were made in the calculations require experimental validation, and discussions are necessary with an end-user before optimizations can be finalized. At this time, there is no plan to further develop this amplifier into space-bound equipment.

The amplifier was tested at 100 Hz in 2018, but high average power operation revealed photoresin residue on the multizone mirror, and repeated optical damage on its HR surface prevented operation at full power. New specification of the multizone mirror was done, and a new lot was provisioned. Characteristics of the amplified beam at 100 Hz will be presented.

4. AMPLIFIER MAIN ASSETS

As mentioned above, the amplifier described here exhibits very low thermal lensing effects. Measurements at 50 Hz showed a focal length continuously larger than 50 m for the thermal lens. When powered on, it reaches full power in 3.9 s and its output beam is very stable, thanks to diode pumping. The output beam is hexagonal in shape, and flat-top in distribution. This distribution is very favorable for frequency conversion and high conversion efficiency of greater than 70% have been achieved with beam having tophat profile [3], [4], [5].

The pumping scheme described Figure 2 not only provides efficient, uniform irradiation of the disk, it presents several valuable advantages. First, in such a system, each diode is imaged over the totality of the hexagonal irradiated area on the disk. Not only is the irradiation very uniform over the hexagon, it remains uniform even if some diodes fail in the stack. As diode stacks age, the overall intensity would decrease, but the beam properties would remain unchanged.

A corollary of this property is that the diode stacks can be shifted in a direction perpendicular to the diode bars without modification of the irradiation pattern on the disk, up to several millimeters. We have demonstrated that when 2 diode stacks are assembled adjacent to each other in front of each disk, they both illuminate the same area uniformly, as long as the bars pitch is no larger than 800 µm. This means that the disks can be powered by 2 separate diode stacks if they are powered independently. The result is pump source redundancy with no drop in efficiency, no change in the beam spatial properties, no additional optical element, and no moving part. The mass increase for pump duplication in the 3D CAD drawing is only 3%, for a large increase of the system lifetime. Indeed, being the only electro-optical element of the amplifier, diode stacks are the most sensitive component to solar radiations, and their duplication could potentially double the system lifetime in space.

5. CONCLUSION

We have refined the design of a 400-mJ amplifier based on thick disks as active mirrors to improve performance at high repetition rate. A 3D CAD drawing of the system has been realized, and modal theory has been applied to analyze its vibration resistance to frequency spectra typical of launch conditions.. The redesigned amplifier has been assembled, and the latest experimental results will be presented.

6. REFERENCES

[1] European patent EP3005498 B1 (2018), CILAS, ArianeGroup

[2] Rapaport Alexandra,Auroux Sandrine, Fretel Emmanuel, Montagne Jean-Eucher, Speiser Jochen, Papayannis Alex, Papadopoulos Dimitri, Tzeremes Georgios, " New 400 mJ Amplifier for Spaceborne Wind Mapping LIDAR", OSA Laser Congress (2020).

[3] Naraniya, Om & Shenoy, Mangalpady & Thyagarajan, K.."Efficiency improvement in MgO:PPLN based optical parametric generation using soft-edge top-hat transverse intensity profile for the pump beam," Optics Communications. 316. 74–79 (2014).

[4] Peng Zhu, Daijun Li, Bingsong Qi, Alexander Schell, Peng Shi, Claus Haas, Shaojun Fu, Nianle Wu, and Keming Du, "Diode end-pumped high-power Q-switched double Nd:YAG slab laser and its efficient near-field second-harmonic generation," Opt. Lett. 33, 2248-2250 (2008).
[5] Bhandari, Rakesh & Taira, Takunori. (2011). Megawatt level UV output from [110] Cr4+:YAG passively Q-switched microchip laser. Optics express. 19. 22510-4.